Sequential crystallization and morphology of triple crystalline biodegradable PEO-*b*-PCL-*b*-PLLA triblock terpolymers

Jordana K. Palacios[a], Agurtzane Mugica[a], Manuela Zubitur[b], Amaia Iturrospe[c], Arantxa Arbe[c], Guoming Liu[d], Dujin Wang[d], Junpeng Zhao[e], Nikos Hadjichristidis[†e] and Alejandro J. Müller[†a,f]

The sequential crystallization of poly(ethylene oxide)-*b*-poly(e-caprolactone)-*b*-poly(L-lactide) (PEO-*b*-PCL-*b*-PLLA) triblock terpolymers, in which the three blocks are able to crystallize separately and sequentially from the melt, is presented. Two terpolymers with identical PEO and PCL block lengths and two different PLLA block lengths were prepared, thus the effect of increasing PLLA content on the crystallization behavior and morphology was evaluated. Wide angle X-Ray scattering (WAXS) experiments performed on cooling from the melt confirmed the triple crystalline nature of these terpolymers and revealed that they crystallize in sequence: the PLLA block crystallizes first, then the PCL block, and finally the PEO block. Differential scanning calorimetry (DSC) analysis further demonstrated that the three blocks can crystallize from the melt when a low cooling rate is employed. The crystallization process takes place from a homogenous melt as indicated by small angle X-Ray scattering (SAXS) experiments. The crystallization and melting enthalpies and temperatures of both PEO and PCL blocks decrease as PLLA content in the terpolymer increases. Polarized light optical microscopy (PLOM) demonstrated that the PLLA block templates the morphology of the terpolymer, as it forms spherulites upon cooling from the melt. The subsequent crystallization of PCL and PEO blocks occurs inside the interlamellar regions of the previously formed PLLA block spherulites. In this way, unique triple crystalline mixed spherulitic superstructures have been observed for the first time. As the PLLA content in the terpolymer is reduced the superstructural morphology changes from spherulites to a more axialitic-like structure.

Introduction

Block copolymers have attracted much attention in the past few decades because they combine polymeric segments of different chemical nature and physical properties.[1] Due to the immiscibility of the building blocks, the polymer chains have the remarkable ability to self-assemble at a molecular level into a wide range of ordered superstructures and unique morphologies. These nanostructured materials can be applied in several fields of interest such as nanotechnology, lithography and optolectronics.[2-3] Since physical properties and final performance are in direct relationship with the overall crystallinity and superstructural morphology of the constituent blocks, crystalline block copolymers have been extensively investigated and several reviews have been published in the past decade.[2, 4-8]

In block copolymers with one or more crystallizable blocks, understanding of the final morphology upon crystallization is complicated since it is influenced by copolymer composition and segregation strength between the blocks. The crystallization process usually competes with phase segregation. Hence, in miscible or weakly segregated block copolymers the crystallization event drives the structure formation and overwrites any previous melt microdomain structure. In contrast, confined crystallization occurs inside the copolymer microdomains in strongly segregated systems. Extensive research has been carried out on the crystallization of miscible or strongly segregated *AB, ABA* and *ABC*-type block copolymers and terpolymers with one or two crystallizable blocks.[2, 5-10] In contrast, the crystallization behavior of triblock terpolymers with three crystallizable blocks is expected to be more complex and, to our knowledge, only three reports have been published dealing with terpolymers that contain three potentially crystallizable blocks.[11-13]

Block copolymers composed of biodegradable and biocompatible polymers, such as poly(L-lactide) (PLLA), poly(e-caprolactone) (PCL) and poly(ethylene glycol)/poly(ethylene oxide) (PEG/PEO), have attracted much attention because of their potential applications in the biomedical field (sutures, bone fixation devices, drug delivery, vesicles, among others).[2, 14-15] Morphology, physical properties, mechanical performance and biodegradation features are strongly governed by crystallization. Several reviews have published on biodegradable or biocompatible block copolymers with double crystalline nature.[2, 7, 9]

PCL-*b*-PLLA diblock copolymers are either miscible or weakly segregated in the melt, according to several publications.[2, 7, 16-22] The presence of phase segregation in the melt has been reported only for specific compositions (typically close to symmetric compositions) and when the segregation strength increases as samples are prepared with higher molecular weights.[17] The segregation strength of a block copolymer depends on the product of the c parameter and the degree of polymerization. Nevertheless, regardless of whether crystallization proceeds from a melt mixed or a weakly segregated melt, the PLLA block crystallization dominates over any pre-existing weak phase segregation in PCL-*b*-PLLA diblock copolymers. Upon cooling from the melt, PLLA block spherulites are formed that template the superstructural morphology. Further cooling to lower temperatures induces the PCL block crystallization within the interlamellar regions of the previously formed PLLA block spherulites. SAXS experiments demonstrated that when the PCL block starts to crystallize, the lamellar PLLA stacks

rearrange to accommodate the newly formed PCL block lamellae. [7, 20-21]

PEO-*b*-PLLA copolymers are most likely miscible in the melt,[18, 23] while PEO-*b*-PCL ones exhibit a complete melt miscibility that has been confirmed by X-ray diffraction[24-27] and rheological measurements.[28]

According to the above, since PCL-*b*-PLLA, PEO-*b*-PLLA and PEO-*b*-PCL are either weakly segregated or miscible, it is expected that PEO-*b*-PCL-*b*-PLLA triblock terpolymers will have a similar behavior, i.e., they will not constitute a strongly segregated block terpolymer system.

Copolymer composition, molecular architecture and block M_w affect the crystallization behavior in block copolymers. A common observation is a decrease in both crystallization and melting temperatures of each block as its content in the copolymer is reduced. This behavior has been reported on diblock copolymers of PLLA with PEO or PCL. For instance, in PEO-*b*-PLLA copolymers, the PLLA melting temperature reduction is caused by a diluent effect of the PEO block. Also, this temperature decreased with the molecular weight.[29] On the other hand, the decrease in the crystallization temperature of PEO or PCL is a consequence of the restriction imposed by the previously crystallized PLLA that confines their crystallization.[14, 29] In fact, a fractioned crystallization[4, 6] phenomenon has been reported on PEO in some PEO-*b*-PLLA diblock copolymers when PEO content was 29 % or lower.[7, 29] If the PEO content is below 20 %, this block is not able to crystallize.[14, 23, 30-32]

In the case of PEO-*b*-PCL diblock copolymers, their crystallization and melting behavior is well documented[33-34] but not easy to elucidate, due to the closeness of both crystallization and melting temperatures of the blocks. As in the aforementioned diblocks copolymers, these temperatures are highly influenced by composition and M_w of each component. The block in higher quantity would crystallize first and melt last. Typically, the crystallization becomes more hindered as the content of the block decreases; and fractionated crystallization events can also occur as a result of confinement.[7, 25] This phenomenon also causes a depression of the melting temperature of the confined block. However, when the diblock copolymer is symmetric (composition close to 50%) a coincident crystallization and melting can occur.

Besides the double crystalline diblock copolymers, analogous *ABA*-type triblock copolymers have also been extensively investigated. Many reports and reviews[9] have been published on PLLA-*b*-PEO-*b*-PLLA,[7, 18, 32, 35-36] PLLA-*b*-PCL-*b*-PLLA[18] and PCL-*b*-PEO-*b*-PCL[37-38] triblock copolymers and, in general, the crystallization behavior is quite similar to the one reported on analogous diblock pairs.

Moreover, the crystalline superstructures observed in both *AB* and *ABA*-type triblock copolymers have been extensively reviewed and include mixed spherulites, concentric spherulites, dendrites, axialites and eutectic crystals.[2, 10, 39-40] Recently, Yang et al.[39] reported that the subsequent crystallization of PEG blocks in PLLA-b-PEG diblock copolymers could change the crystalline structure of PLLA crystals, and the extent of this change is determined by the crystallization temperature of the PLLA block.

Attempts to achieve a fully triple crystalline triblock terpolymer have been done in the past. Some of us, synthesized a PE-*b*-PEO-*b*-PCL triblock terpolymer in which the central block was not able to crystallize, mainly due to topological restrictions imposed by the previously crystallized PE and PCL blocks.[11] Later, Sun et al. reported the synthesis of triblock and pentablock terpolymers composed of PCL, PLLA and PEG.[12] The authors reported that the terpolymers were crystalline from DSC analysis and WAXS experiments performed at room temperature. However, the main focus of their study was on the self-assembly ability of the terpolymers to form nanoparticles in aqueous solution. Similar terpolymers have been used as amphiphilic materials that can form micellar structures[41] and have been tested in drugs release applications.[12] Another reported application for similar terpolymers is to template phenolic resins while curing.[42] More recently, Chiang et al.[13] reported trilayered single crystals of PEO-*b*-PCL-*b*-PLLA terpolymers in thin films obtained by solvent-induced crystallization.

In this work, we report the morphology and crystallization of two biocompatible PEO-*b*-PCL-*b*-PLLA triblock terpolymers, in which the three blocks are able to crystallize separately and sequentially. The one-pot sequential polymerization of these terpolymers has been reported in a previous work by some of us.[43] The triple crystalline nature of the triblock terpolymers, as well as their melt miscibility, sequential crystallization and superstructural morphology are examined here by employing small angle and wide angle X-Ray scattering (SAXS, WAXS), differential scanning calorimetry (DSC) and polarized light optical microscopy (PLOM). The study of these novel triple crystalline PEO-*b*-PCL-*b*-PLLA triblock terpolymers provides new fundamental insights on the formation of mixed triple crystalline spherulites and sequential crystallization of triblock terpolymers.

Experimental

Materials

The PEO-*b*-PCL-*b*-PLLA triblock terpolymers were synthesized, as previously described, by one-pot sequential organocatalytic ring-opening polymerization of ethylene oxide (EO), ε-caprolactone (CL) and L-lactide (LLA) using a phosphazene base, 1-tert-butyl-2,2,4,4,4-pentakis(dimethylamino)-2λ^5,4λ^5-catenadi(phosphazene) (t-BuP_2), as a single catalyst for the three monomers.[43] After the polymerization of the second monomer (CL), the reaction solution was divided into two approximately equal parts. Then, different amount of LLA was added into each part to form the third block. In this way, it was ensured that the triblock terpolymers have the same lengths of PEO and PCL blocks (4600 g mol^{-1} for PEO and 6800 g mol^{-1} for PCL), and different lengths of PLLA blocks (4700 and 8500 g mol^{-1}, respectively). Size exclusion chromatography (SEC) revealed that the triblock terpolymers had relatively low molecular weight distributions (ÐM < 1.20), and the nuclear magnetic resonance spectra (1H NMR) represented all the characteristic signals of the expected macromolecular structure, including the main bodies of the

three blocks, end groups and groups linking different blocks. Due to the use of PEO standards, the number-average molecular weight (M_n) of the PEO block obtained by SEC analysis was considered the absolute value, which was then used to calculate the M_n*s* of the other blocks from the 1H NMR spectra (values given above). The two triblock terpolymer samples used in this study are named herein as $PEO_{29}PCL_{42}PLLA_{29}^{16.1}$ and $PEO_{23}PCL_{34}PLLA_{43}^{19.9}$. The subscript numbers represent the weight fractions of the blocks calculated from the M_n*s* and the superscript numbers, the molecular weight of the entire terpolymer.

Small angle X-Ray scattering (SAXS)

The large-scale structure was investigated by Small Angle X-Ray Scattering (SAXS). Experiments were performed on a Rigaku 3-pinhole PSAXS-L equipment operating at 45 kV and 0.88 mA. The MicroMax-002+ X-Ray Generator System composed by a microfocus sealed tube source module and an integrated X-Ray generator unit produces CuK_α transition photons of wavelength λ = 1.54 Å. The scattered X-Rays are detected on a two-dimensional multiwire X-Ray Detector (Gabriel design, 2D-200X). With a 200 mm diameter active area, this gas-filled proportional type detector offers ca. 200 micron resolution. The azimuthally averaged scattered intensities were obtained as a function of wave vector *q* ($q = 4\pi * \sin\theta/\lambda$, where 2θ is the scattering angle). Reciprocal space calibration was done using silver behenate as standard. The samples were placed in a Linkam Scientific Instruments THMS 600 temperature controller (range: -196 to 600 °C, stability < 0.1 °C) at a distance of 2 m from the detector, covering a q-range: $0.1 \leq q \leq 1.5$ nm^{-1}. Flight path and sample chamber were under vacuum. Experiments were conducted at room temperature, 80 ºC and 140 ºC with measuring times of 5 min.

Differential scanning calorimetry (DSC)

A Perkin Elmer DSC Pyris 1 was employed to perform DSC measurements of the triblock terpolymers. Samples of approximately 3 mg were encapsulated in aluminum pans and tested under ultra-high purity nitrogen atmosphere. The instrument was previously calibrated with an indium standard. The thermal program employed for all samples was as follows: an initial heating run from 25 to 160 °C at 20 °C min^{-1}, keeping the sample for 3 min at that temperature to erase the thermal history, followed by a cooling scan down to -20 °C at 1 °C min^{-1}, and a second heating scan up to 160 °C at 20 °C min^{-1}.

Wide angle X-Ray scattering (WAXS)

In-situ WAXS measurements were carried out at the beamline BL16B1 in the Shanghai Synchrotron Radiation Facility (SSRF). The wavelength of the radiation source was λ = 1.2398 Å. Scattering patterns were collected using a MAR 165 detector with a resolution of 2048×2048 pixels (pixel size: 79×79 μm^2). The sample-to-detector distance was 178 mm, and the effective scattering vector *q* range was 5~21 nm^{-1}. The temperature profile was controlled by a Linkam TST350 stage. To avoid degradation, all experiments were carried out under nitrogen atmosphere. The triblock terpolymer samples were first heated to 160 ^{O}C and kept at that temperature for 3 min to erase possible thermal history. During cooling at 5 ºC min^{-1}, scattering patterns were collected in-situ to monitor the non-isothermal crystallization process. The acquisition time for each pattern was 9 s, yielding a temperature resolution of 1 ºC. All the X-ray patterns were corrected for detector noise, air scattering and sample absorption. The two dimensional scattering patterns were integrated radially to one dimensional intensity profiles using the program Fit2D.

Morphological observations

The crystalline morphology of the triblock terpolymers was observed by polarized light optical microscopy (PLOM). Films were prepared by melting the sample between a glass slide and a cover slip employing a Mettler Toledo FP82HT hot stage plate. Samples were observed in a Leitz Aristomet microscope with crossed polarizers and making use of λ wave plate to determine the sign of the spherulites. The thermal protocol applied was as follows: once the sample was melted at 160 ºC inside the hot stage, it was kept at this temperature for 3 min. Then, it was quickly cooled down sequentially to the isothermal crystallization temperature of each block.

Results and discussion

SAXS characterization of the PEO-b-PCL-b-PLLA triblock terpolymers

SAXS experiments of both triblock terpolymers were performed at room temperature (RT), 80 and 140 ºC and the resulting patterns are shown in Fig 1. SAXS patterns were taken during heating, so the disappearance of scattering peaks is a result of the melting of each block in the terpolymer. At 140 ºC, both triblock terpolymers are in the melt state, according to previous DSC measurements (see also below). Fig 1a shows that no reflection was observed at 140 ºC for the $PEO_{29}PCL_{42}PLLA_{29}^{16.1}$ sample while the other triblock terpolymer exhibits a single very broad and weak reflection at this temperature (Fig 1b). Both observations indicate that the terpolymers are most likely miscible in the melt. The broad reflection of the $PEO_{23}PCL_{34}PLLA_{43}^{19.9}$ sample at 140 ºC can be adscribed to a correlation hole effect[21, 44-45] that produces broad signals in the scattering pattern of block copolymers with a homogeneous melt morphology. Similar observations have been previously reported in literature for miscible or weakly segregated di and triblock copolymers[20-21]

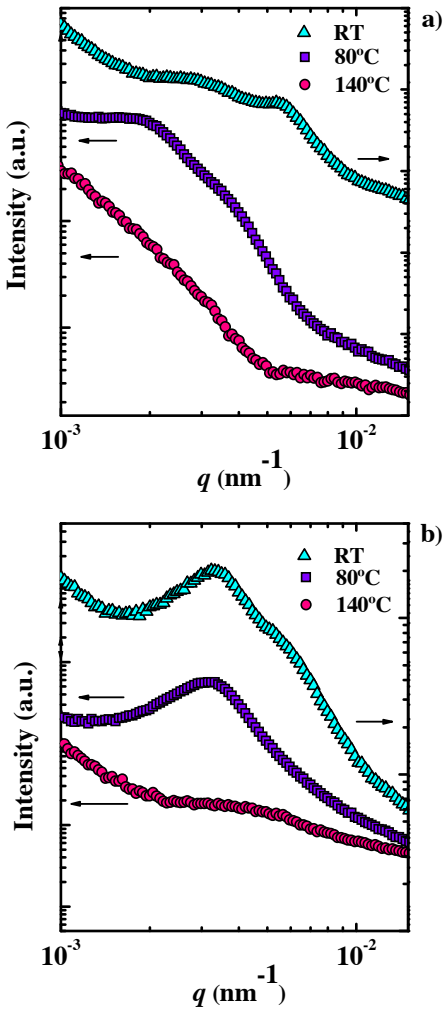

Fig 1. SAXS patterns taken at different temperatures on heating of a) $PEO_{29}PCL_{42}PLLA_{29}$[16.1] and b) $PEO_{23}PCL_{34}PLLA_{43}$[19.9]

For instance, a homogeneous melt have been detected by SAXS for PCL-*b*-PLLA,[20-21, 46] PEO-*b*-PLLA[47] and PCL-*b*-PEO copolymers.[7] In diblock copolymers, microphase segregation in the melt can be predicted by calculating the segregation strength, i.e., the product of *cN*, on the basis of the mean-field theory.[48-49] The parameter *c* is the Flory-Huggins interaction parameter and *N* the polymerization degree. According to this theory, if the *cN* value is ≤ 10 the entropic terms prevail and the system will exhibit a disorder-homogeneous melt. Since our samples are *ABC*-type triblock terpolymers, estimating their miscibility through this theory becomes more complicate because, to our knowledge, experimental determination of the *c* value for any of the diblocks in the terpolymer has not been reported so far. Thus, a rough estimation of *c*[16, 50-51] and *cN* parameter for each pair of blocks *AB*, *BC* and *AC* has been calculated using the solubility parameters of PEO, PCL and PLLA reported in the literature.[16 51] The values obtained are compiled in

Table 1. The low *cN* values (≤ 10) of the pairs in both samples could be used as an approximate indication of a low melt-segregation level in the triblock. Thus, although the calculated values might not fully represent the interactions in the whole triblock terpolymer, it would be expected that PEO, PCL and PLLA blocks would be miscible or weakly segregated in the melt. These calculations are in line with our SAXS results and support our contention that the two triblock terpolymers employed here are miscible in the melt. As already mentioned in the introduction, PEO-*b*-PCL[24-28] and PEO-*b*-PLLA[7, 18, 36, 47, 51-52] diblock copolymers are reported to be miscible in the melt,[7] while PCL-*b*-PLLA copolymers are known for exhibiting either a miscible[16-17, 20-21, 46, 53] or weakly segregated[17-19, 22] behavior, depending on composition and PLLA block M_w.

SAXS scattering peaks observed at room temperature and 80 ºC suggest a periodic lamellar microdomain structure with long-range order.[33] For instance, in PEO-*b*-PCL diblock copolymers, their structure consists of alternating crystalline lamella of each component with amorphous layers in between.[33] This alternating lamellar structure has also been reported on PLLA-*b*-PEO / PLLA-*b*-PEG and PLLA-*b*-PCL copolymers (see[2, 7] and references therein), which are all miscible or weakly segregated in the melt. Thus, it Is possible that a similar but even more complicated morphology (i.e., with the presence of three different lamellar crystal types within the spherulites) exists in these terpolymers. The existence of mixed spherulites will be demonstrated below by Polarized Light Optical Microscopy (PLOM) experiments.

Non-Isothermal crystallization of PEO-b-PCL-b-PLLA triblock terpolymers evaluated by DSC and WAXS.

The morphology of the samples is in direct relationship with their thermal behavior. Thus, DSC analysis was performed in order to evaluate if the blocks in the terpolymers are able to crystallize under standard cooling conditions. First of all, Fig 2 exhibits the DSC heating scan of the samples as-synthesized. Three clear endothermic peaks are observed in both samples. Since the typical melting temperatures of PLLA as homopolymer and in block copolymers are between 80 and 180 ºC,[52] the highest temperature peak is assigned to the melting of PLLA crystals. Then, the other two lower temperature peaks must correspond to the melting of PEO, PCL, or both PEO/PCL crystals.

Table 1. Values of *c* and segregation strength parameter *cN* calculated for different diblock copolymer pairs at different temperatures. Such diblock copolymer pairs can be considered precursors or parts of the chain of thePEO-*b*-PCL-*b*-PLLA triblock terpolymers

Sample	Temperature (ºC)	PEO-PCL		PCL-PLLA		PEO-PLLA	
		c	*cN*	*c*	*cN*	*c*	*cN*
$PEO_{29}PCL_{42}PLLA_{29}^{16.1}$	160	-	-	$1.86x10^{-2}$	2.32	$2.90x10^{-4}$	0.04
	90	$2.81x10^{-2}$	3.59	$2.22x10^{-2}$	2.77	$3.46x10^{-4}$	0.05
	50	$3.15x10^{-2}$	4.01	-	-	-	-
	41	$3.24x10^{-2}$	4.14	$2.56x10^{-2}$	3.20	$4.00x10^{-4}$	0.05
	25	$3.42x10^{-2}$	4.37	$2.70x10^{-2}$	3.37	$4.22x10^{-4}$	0.06
$PEO_{23}PCL_{34}PLLA_{43}^{19.9}$	160	-	-	$1.86x10^{-2}$	3.30	$2.90x10^{-4}$	0.05
	90	$2.81x10^{-2}$	3.59	$2.22x10^{-2}$	3.94	$3.46x10^{-4}$	0.06
	50	$3.15x10^{-2}$	4.01	-	-	-	-
	41	$3.24x10^{-2}$	4.14	$2.56x10^{-2}$	4.55	$4.00x10^{-4}$	0.07
	25	$3.42x10^{-2}$	4.37	$2.70x10^{-2}$	4.79	$4.22x10^{-4}$	0.08

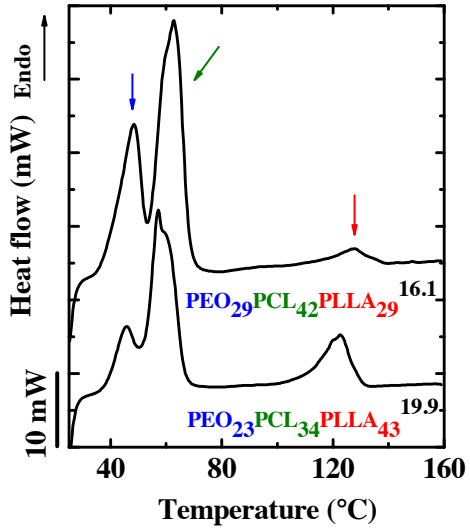

Fig 2. First DSC heating scans of as obtained reactor powders of the indicated triblock terpolymers at 20 ºC min^{-1}.

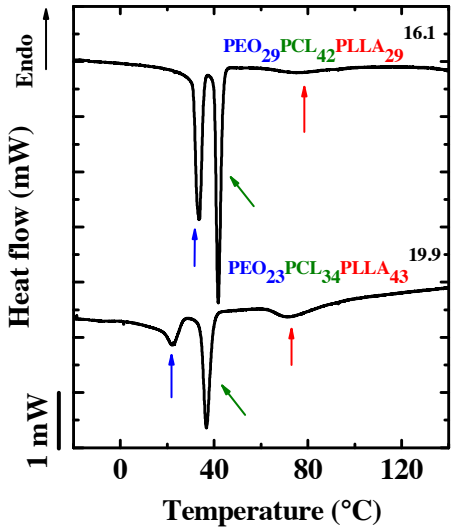

Fig 3. DSC cooling scans at 1 ºC min^{-1} after melting at 160 ºC for 3min.

After melting, the subsequent cooling scans were recorded at 1 ºC min^{-1}. Several tests were carried out to establish the ideal cooling rate to achieve the crystallization of the blocks. From this analysis, a low cooling rate is needed to accomplish this goal (see supplementary information S1). Fig 3 shows three well defined exothermic peaks that are due to the crystallization from the melt of the blocks. The PLLA block crystallizes first upon cooling from the melt at around 70ºC. After PLLA block crystallization, upon further cooling, the following blocks to crystallize are either PEO or PCL. Similar results have been reported recently in similar PEO-*b*-PCL-*b*-PLLA terpolymers obtained by a different synthetic pathway.[13]

In PEO-*b*-PCL diblock copolymers the sequence of crystallization depends on copolymer composition. For instance, when PCL is the major component, this block crystallizes first and then the PEO block. The opposite behavior is observed when the PEO content is higher.[33] Thus, further analyses by WAXS are needed in order to properly identify the order in which PCL and PEO blocks crystallize from the melt.

The second DSC heating scans of the triblock terpolymers (after the cooling shown in Fig 3) are shown in Fig 4. The melting of the PLLA block clearly takes place around 120 ºC, identified by a broad endothermic peak with a minor low-temperature shoulder. This shoulder is a common observation and it has been reported before for PLLA homopolymers. Such double melting behaviour has been adscribed to a recrystallization-melting mechanism leading to the formation of a more stable crystalline phase.[54-57] This typical behavior has also been observed in PLLA-containing diblock copolymers with PCL[53] and PEO.[29, 51, 58] Other works on PLLA based diblock[17, 54] and *ABA*-type triblock[18] copolymers did not observe this minor shoulder.

Another interesting observation is the absence of the typical cold crystallization peak of PLLA block during heating, which has been usually reported for PLLA block copolymers.[20-21, 53-54] The appearance of this peak depends on the length of the PLLA block, copolymer composition and cooling conditions. Since the

cooling rate employed here was very low (1 ºC min^{-1}), the PLLA block is able to crystallize until saturation under this condition and additional crystallization does not occur during the heating scan.

In our triblock terpolymers, the PEO and PCL crystals melt between 40 and 60 ºC. A double peak endotherm located between these temperatures indicates the melting of these blocks, but which one occurs first will be elucidated by WAXS analysis below.

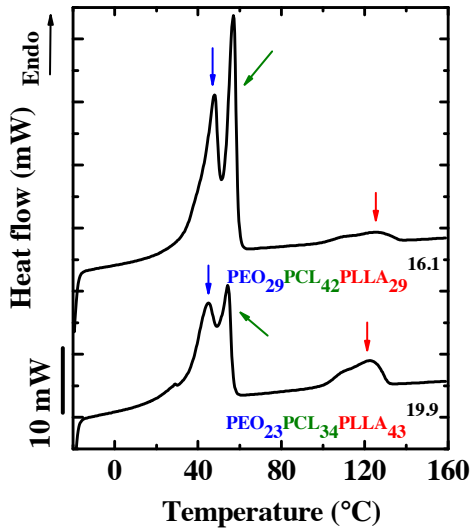

Fig 4. Subsequent DSC heating scans at 20 ºC min^{-1} after cooling at 1 ºC min^{-1} (shown in Fig 3).

The local structure of both samples was investigated by WAXS experiments performed on cooling and the resulting patterns are shown in Fig 5 and Fig 6. The patterns confirm beyond any doubt the triple crystalline nature of these novel *ABC*-type triblock terpolymers. The reflections pointed out in those figures clearly reflect that each block crystallizes separately in an independent unit-cell structure. The PEO, PCL and PLLA crystals co-exist together in the terpolymer at low temperatures. The indexation reported in **¡Error! No se encuentra el origen de la referencia.** agrees well with the assignments widely published in the literature for PEO, PCL and PLLA crystals within diblock copolymers.[18, 20-21, 34, 51, 53, 59]

Taking for example the $PEO_{29}PCL_{42}PLLA_{29}^{16.1}$ terpolymer (see Fig 5), the two peaks at 11.73 and 13.37 nm^{-1} correspond to 100/200 and 203 reflections of the α form of PLLA. The very strong peak and the small shoulder close to it located at 14.96 and 15.37 nm^{-1} belong to 110 and 111 reflections of PCL respectively, along with the 200 reflection at 16.56 nm^{-1}. And, since the PLLA 203 peak coincides with the PEO 120 reflection, the evidence that the PEO block is able to crystallize is the small shoulder that belong to 112/032/132/212 reflection of PEO crystals located at 16.33 nm^{-1}. The $PEO_{23}PCL_{34}PLLA_{43}^{19.9}$ terpolymer also displays the 010 and 210 PLLA reflections at 10.44 and 15.56 nm^{-1}, respectively.[18, 20-21, 34, 51, 53, 59] The values of the 2θ angles reported in Table 2 were obtained from the scattering vector q and the typical CuK_α radiation (λ = 1.54 Å). According to literature, PLLA and PCL crystallize in an orthorhombic system while the PEO does it in a monoclinic structure.[34, 58]

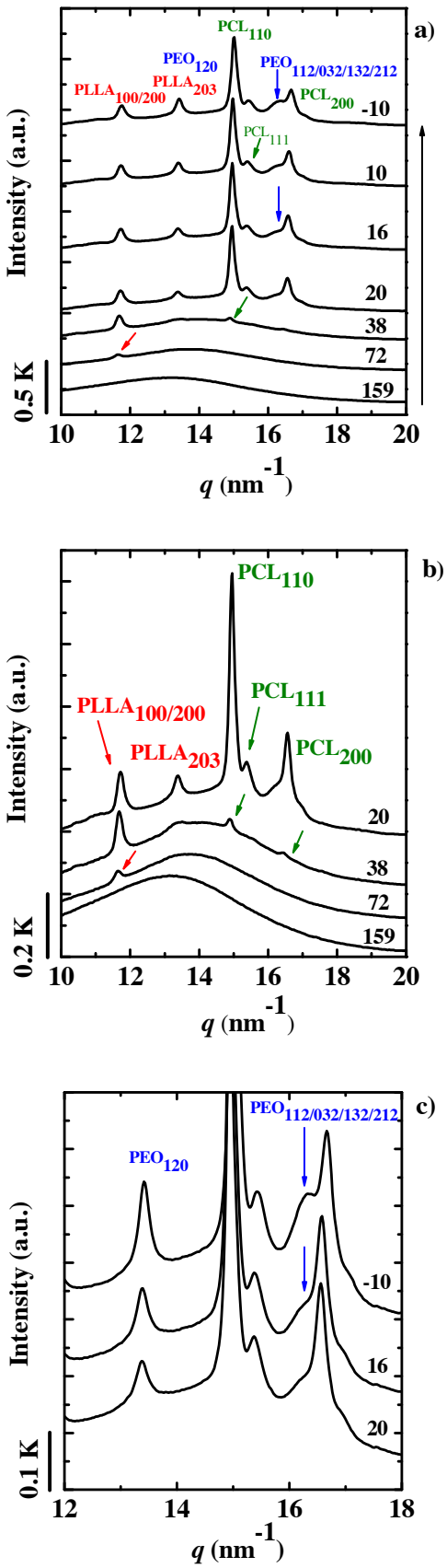

Fig 5. a) WAXS pattern taken at different temperatures during cooling from the melt at 5 ºC min^{-1} of $PEO_{29}PCL_{42}PLLA_{29}^{16.1}$. Peak assignment and structural features of each block are indicated in more detail in: b) PLLA and PCL and c) PEO.

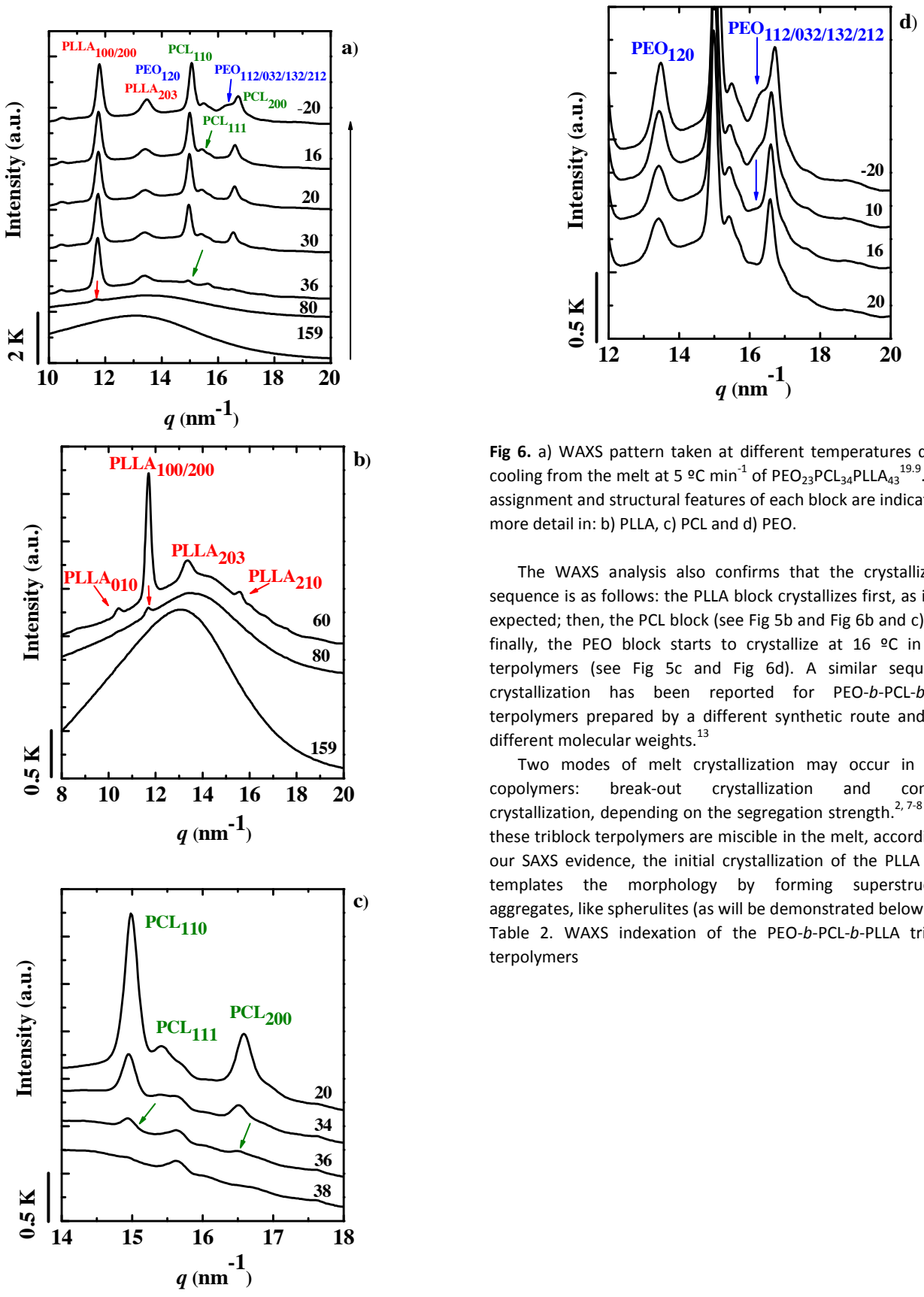

Fig 6. a) WAXS pattern taken at different temperatures during cooling from the melt at 5 ºC min^{-1} of $PEO_{23}PCL_{34}PLLA_{43}$[19.9]. Peak assignment and structural features of each block are indicated in more detail in: b) PLLA, c) PCL and d) PEO.

The WAXS analysis also confirms that the crystallization sequence is as follows: the PLLA block crystallizes first, as it was expected; then, the PCL block (see Fig 5b and Fig 6b and c), and, finally, the PEO block starts to crystallize at 16 ºC in both terpolymers (see Fig 5c and Fig 6d). A similar sequential crystallization has been reported for PEO-*b*-PCL-*b*-PLLA terpolymers prepared by a different synthetic route and with different molecular weights.[13]

Two modes of melt crystallization may occur in block copolymers: break-out crystallization and confined crystallization, depending on the segregation strength.[2, 7-8] Since these triblock terpolymers are miscible in the melt, according to our SAXS evidence, the initial crystallization of the PLLA block templates the morphology by forming superstructural aggregates, like spherulites (as will be demonstrated below).[2, 7]

Table 2. WAXS indexation of the PEO-*b*-PCL-*b*-PLLA triblock terpolymers

Sample	Reflections	q_{max} (nm^{-1})	D (nm)	2θ [a] (º)
$PEO_{29}PCL_{42}PLLA_{29}^{16.1}$	$PLLA_{100/200}$	11.73	0.54	16.5
	$PLLA_{203}$	13.37	0.47	18.9
	PCL_{110}	14.96	0.42	21.1
	PCL_{111}	15.37	0.41	21.7
	PCL_{200}	16.56	0.38	23.4
	PEO_{120}	13.41	0.47	18.9
	$PEO_{112/032/132/212}$	16.33	0.38	23.1
$PEO_{23}PCL_{34}PLLA_{43}^{19.9}$	$PLLA_{010}$	10.44	0.60	14.7
	$PLLA_{100/200}$	11.69	0.54	16.5
	$PLLA_{203}$	13.35	0.47	18.9
	$PLLA_{210}$	15.56	0.40	22.0
	PCL_{110}	14.98	0.42	21.2
	PCL_{111}	15.42	0.41	21.8
	PCL_{200}	16.58	0.38	23.5
	PEO_{120}	13.48	0.47	19.0
	$PEO_{112/032/132/212}$	16.36	0.38	23.2

[a] The values of 2θ correspond to the typical CuK_α radiation (λ = 1.54 Å).

The previously crystallized PLLA block will restrict the crystallization of the other two blocks creating an alternating lamellar template that confines the amorphous PLLA chains together with the molten PCL and PEO blocks. Despite interlamellar confinement in the intra spherulitic domains of PLLA block spherulites, Fig 5b and Fig 6b and c indicate that the PCL block can crystallize upon further cooling.

In PEO-*b*-PCL diblock copolymers the order of crystallization also depends on the copolymer composition. He et al. found that PCL crystallizes first when the PCL content was 43 % or higher, but if the PCL content is 36 % or less the PEO is the one who crystallizes first.[33] Similar results were reported by Sun et al.[60] and Wei et al.[38] in PEO-*b*-PCL diblock and PCL-*b*-PEG-*b*-PCL triblock copolymers, respectively. Hence, the main reason for the order of crystallization observed in our triblock terpolymers is the larger PCL content within them.

After the PCL block crystallization, the PEO block chains have no other choice but to crystallize inside the limited spaces left in between PLLA block and PCL block lamellae. The confinement imposed by these two previously formed lamellar crystals will hinder its crystallization, and this is the reason why the intensity of the PEO reflections in both triblock terpolymers are not sharp. WAXS experiments during heating allows assigning the melting behavior shown in Fig 4 to the sequential fusion of all three corresponding blocks. Patterns exhibited in Fig 7 clearly demonstrate that, in both triblock terpolymers, PEO crystals melt first, as indicated with the blue arrow (see color figure for reference), then PCL and finally the PLLA block.

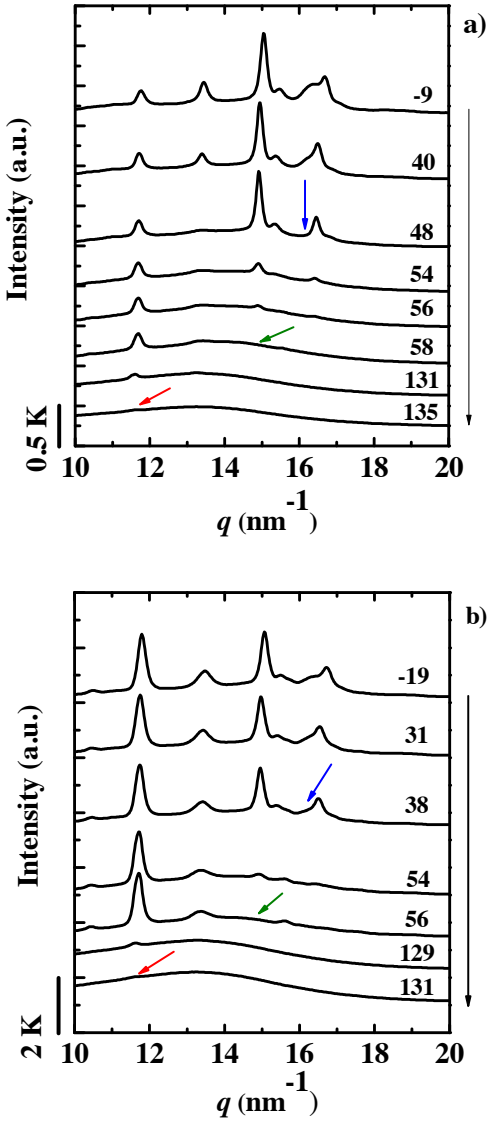

Fig 7. WAXS pattern taken at different temperatures during subsequent heating at 5 ºC min^{-1} of a) $PEO_{29}PCL_{42}PLLA_{29}^{16.1}$ and b) $PEO_{23}PCL_{34}PLLA_{43}^{19.9}$.

The results of our WAXS analysis, allows proper assignment of the thermal transitions observed by DSC to each the corresponding block. We have assigned a color code (in the web version of our manuscript), to easily identify the crystallization and melting of each block in the DSC traces presented in Fig 2, 3 and 4 and in all WAXS diffractograms above: red for PLLA block, green for PCL block and blue for PEO block. The characteristic thermal properties obtained by DSC are presented in Table 3, 4 and 5.

Table 3. Thermal properties of the triblock terpolymers obtained from DSC 1st heating scan at 20 ºC min^{-1}.

Sample	T_m PEO^{1st} (°C)	DH_m PEO^{1st} (J/g)	T_m PCL^{1st} (°C)	DH_m PCL^{1st} (J/g)	T_m PLLA^{1st} (°C)	DH_m PLLA^{1st} (J/g)
PEO29PCL42PLLA2916.1	48.4	102	62.8	66	127.5	23
PEO23PCL34PLLA4319.9	45.8	46	57.2	104	122.5	33

Table 4. Thermal properties of the triblock terpolymers obtained from DSC cooling scan at 1 ºC min^{-1}.

Sample	T_c PEO (°C)	DH_c PEO (J/g)	T_c PCL (°C)	DH_c PCL (J/g)	T_c PLLA (°C)	DH_c PLLA (J/g)
PEO29PCL42PLLA2916.1	33.5	-108	41.7	-73	75.0	-16
PEO23PCL34PLLA4319.9	22.1	-53	36.7	-63	72.3	-22

Table 5. Thermal properties of the triblock terpolymers obtained from DSC 2nd heating scan at 20 ºCmin^{-1}.

Sample	T_m PEO^{2nd} (°C)	DH_m PEO^{2nd} (J/g)	T_m PCL^{2nd} (°C)	DH_m PCL^{2nd} (J/g)	T_m PLLA^{2nd} (°C)	DH_m PLLA^{2nd} (J/g)
PEO29PCL42PLLA2916.1	48.0	126	56.9	66	112.0 - 124.5	20
PEO23PCL34PLLA4319.9	45.0	112	54.2	45	112.1 - 121.8	28

Comparing thermal properties from WAXS and DSC, the results follow a similar general trend, in spite of the fact that they were conducted at different cooling and heating rates. The PLLA block in the triblock terpolymers presented here crystallizes around 70 ºC. Typical melt crystallization temperatures of PLLA blocks in miscible or weakly segregated diblock copolymers are between 80 and 115 ºC.[7, 20-21, 29, 51, 53-54] A similar situation is observed with the melting point of the PLLA block, it is lower in the triple crystalline triblock terpolymers than in the diblock copolymers previously studied in the literature. In partially miscible block copolymers both PLLA crystallization and melting temperatures decrease when the PLLA content is lower, as a result of a diluent effect of the molten PEO and PCL chains or for compositions where PLLA is a minor component (less than 20%) a confinement effect can also lead to lower crystallization temperatures. This has been the most common observation in PLLA-*b*-PCL[7, 9, 20, 46, 53-54] and PLLA-*b*-PEO[7, 14, 18, 29, 51] diblock copolymers.

The crystallization and melting enthalpies of the PLLA block are highly reduced in the triblock terpolymers, as compared to analogous PLLA-b-PCL diblock copolymers reported previously. For example, $L_{44}C_{56}$[25] and $L_{55}C_{45}$[18] have PLLA ΔH_m values of 82 and 69 J/g respectively,[54] while in the triblock terpolymers those values are reduced to 20 and 28 J/g (see Table 5). Also, PLLA ΔH_c and ΔH_m values in the triblock slightly reduce as the PLLA content reduces. These results indicate that the crystallization ability of the PLLA block is affected by the presence of the two molten covalently bonded PCL and PEO blocks.

The PCL block crystallization and melting temperatures decrease as its content in the triblock terpolymers reduces, as it was expected (see Table 4 and Table 5). The crystallinity values follow a similar trend. Comparable results have been reported by Castillo et al. in PLLA-*b*-PCL diblock copolymers.[54] The reduced crystallinity of the PCL block accounts for the restriction imposed by the previous crystallization of the PLLA block that limits the PCL block lamellae to form in between the lamellar stacks of PLLA and the amorphous phase of the triblock terpolymer.

Finally, PEO is the last block to crystallize. Thus, its crystallization ability will be affected by the previous crystallization of both PLLA and PCL blocks. Nevertheless, the crystallization temperature of the PEO block in both terpolymers is relatively high, a fact that could be due to the nucleating actions of both PLLA and PCL crystals. This means that the PEO block is not undergoing the classical crystallization in confined isolated domains where typically crystallization temperatures can be depressed to values below -30 ºC as nucleation changes from heterogeneous to homogeneous and dominates overall crystallization kinetics (see references[4, 6, 8]).

Despite the crystallization temperature of the PEO block is not significantly affected, its degree of crystallinity is much reduced as compared to analogous PEO chains of equivalent lengths in diblock copolymers or even in homopolymers.[29, 33] This is probably a result of a slower crystallization kinetics of the PEO block (the last to crystallize upon cooling) when it is a part of the triple crystalline triblock terpolymer.

Morphology of the PEO-b-PCL-b-PLLA triblock terpolymers

Solid-state morphology of block copolymers is a reflection of their composition, crystallization behavior, miscibility level and the degree of microphase separation driven by the crystallization process.[5] Polarized light optical microscopy

(PLOM) observations have been performed on cooling from the melt in order to detect the sequential crystallization and superstructural organization of the terpolymers.

Fig 8 exhibits the morphology of both terpolymers as a function of selected temperatures at which each block crystallizes according to DSC and WAXS. First, the melt was quenched to 100 ºC. At this temperature the PLLA block crystallizes, while the other two blocks remain molten. Secondly, a quench was made to 39 ºC, a temperature at which PCL can crystallizeand lastly, a final quench was carried out to room temperature where the PEO block can also crystallize.

At 100 ºC (a temperature at which both PCL and PEO are in the melt), although not very well-defined, a spherulitic-type morphology is observed for the terpolymer with higher PLLA content (i.e., $PEO_{23}PCL_{34}PLLA_{43}^{19.9}$). In the case of the PLLA block within $PEO_{29}PCL_{42}PLLA_{29}^{16.1}$, the superstructural texture is more open and resembles an axialitic-type morphology. PLLA block crystalline lamellae grow radially and form a spherulitic (or axialitic) morphology with a diffuse Maltese cross pattern. With the aid of a first-order retardation plate (λ plate), the position of the observed colors indicate the negative optical sign of the spherulites. The sign of the birefringence means that the highest refractive index is tangential and coincides with the chain direction.[21, 61]

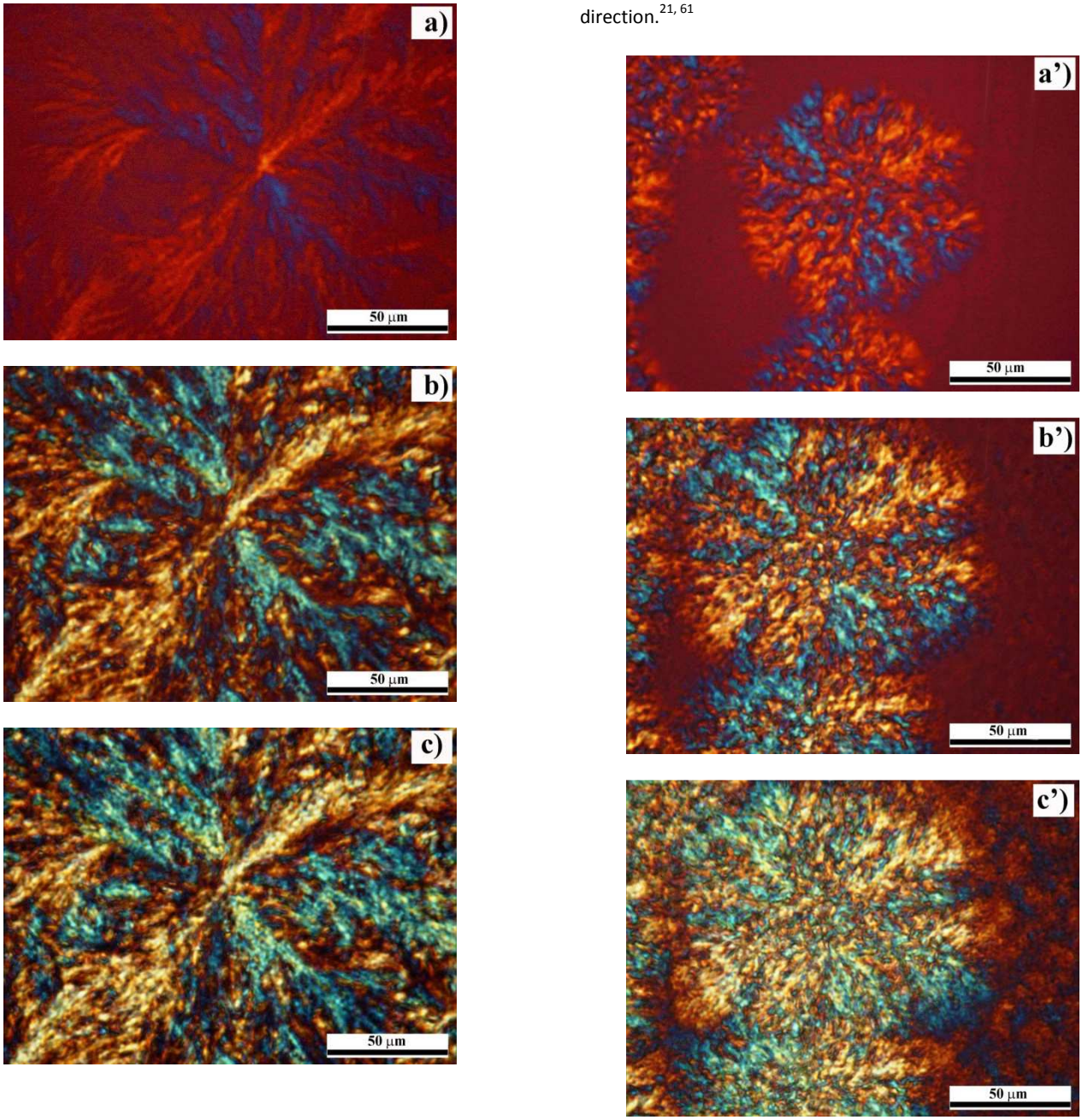

Fig 8. PLOM Micrographs taken at a) a') 100 ºC, b) b') 39 ºC and c) c') room temperature of $PEO_{29}PCL_{42}PLLA_{29}^{16.1}$ (left side) and $PEO_{23}PCL_{34}PLLA_{43}^{19.9}$ (right side). Scale bar 50 μm.

Fig 8 shows that the superstructure formed by PLLA in both triblock terpolymers is irregular and that banding extinction patterns are not observed. In block copolymers, the morphological evolution is influenced by the sample thickness, crystallization temperature and block composition.[2, 7, 10, 47] In many PEO-*b*-PCL, PCL-*b*-PLLA and PEO-*b*-PLLA diblocks copolymers, morphological changes with temperature and composition have been observed: from well-defined Maltese cross spherulites and concentric spherulites to spherulites with continuous banding extinction patterns.[29, 33, 47, 51, 53] For instance, PEO-*b*-PLLA diblock copolymers with PLLA content between 71 and 32 % exhibit PLLA banded spherulites.[52] However, based on the observations of Huang et al.[51] in the same diblock copolymers, the branching morphology developed as PLLA content in the terpolymers is lower (see Fig 8a, left) might be a result of the richer PCL-PEO amorphous phase that surrounds the proximity of the PLLA lamellae and disturbs further growth in their immediate vicinity.[51] Hence, the microphase separation driven by PLLA block crystallization is affected by the proportion of the three phases in the terpolymers.

The PLLA block crystalline superstructure created at 100 ºC templates the morphology for the subsequent crystallization of the PCL and PEO blocks. Fig 8b and b' shows that PCL crystallization takes place at 39 ºC without altering significantly the superstructure of the previously crystallized PLLA block. The spherulities remain negative. However, the magnitude of the birefringence changes. Clear color changes and a new intense brightness account for the newly formed PCL block lamellar crystals within the PLLA block spherulite. Such intraspherulitic crystallization occurs within the interlamellar regions and as a result mixed spherulites are formed. The interlamellar regions are composed of a mixture of PLLA, PCL and PEO chains in the amorphous state. When the sample is quenched again to room temperature, quadrant colors become even lighter and brighter as a result of the PEO block crystallization inside the intra-spherulitic regions (see Fig 8c and c'). The whole crystallization sequence would be better appreciated in a small video available in supplementary information S2. These observations in the $PEO_{29}PCL_{42}PLLA_{29}^{16.1}$ and $PEO_{23}PCL_{34}PLLA_{43}^{19.9}$ triblock terpolymers are very similar to those reported on PCL-*b*-PLLA[7, 20-21, 53] and PEO-*b*-PLLA[14, 29, 36] diblock copolymers. However, in the terpolymer case, unique triple crystalline superstructure are formed with potentially very interesting properties.

Further evidences of the periodic lamellar structure of these micro domains are obtained from SAXS experiments. Table 6 reports the long period distance L calculated from the q values at the maxima observed at room temperature, in which the three blocks are crystallized, and at 80 ºC, where only the PLLA crystals are present. At room temperature, two maxima are detected in both triblock terpolymers, associated to two average long periods in the sample, while only one maximum is observed for the $PEO_{23}PCL_{34}PLLA_{43}^{19.9}$ at 80 ºC.

At room temperature both copolymers have very similar long period values, thus the increase on the PLLA block M_w does not significantly disturb the complex triple lamellar structure present in the terpolymers. However, when temperature is increased to 80 ºC, *L* increases, as a result of the melting of both PEO and PCL block lamellae. After melting, the amorphous layer thickness becomes wider. This result is clearer in the $PEO_{29}PCL_{42}PLLA_{29}^{16.1}$ triblock terpolymer.

Table 6. Long period values *L* of the $PEO_{29}PCL_{42}PLLA_{29}^{16.1}$ and $PEO_{23}PCL_{34}PLLA_{43}^{19.9}$ triblock terpolymers measured at room temperature and 80 ºC

Sample	Temperature (ºC)			
	RT		80	
	q_{max} (A^{-1})	*L* (nm)	q_{max} (A^{-1})	*L* (nm)
$PEO_{29}PCL_{42}PLLA_{29}^{16.1}$	0.0379	16.6	0.0211	29.8
	0.0566	11.1	0.0350	17.9
$PEO_{23}PCL_{34}PLLA_{43}^{19.9}$	0.0369	17.0	0.0341	18.4
	0.0597	10.5	-	-

Conclusions

The sequential crystallization of PEO-*b*-PCL-*b*-PLLA triblock terpolymers was studied by DSC, WAXS, PLOM and SAXS. During the DSC cooling scans at 1 ºC min^{-1}, the three blocks are able to crystallize separately. Subsequent DSC heating scans reveal the melting transition associated to each block. The sequential crystallization followed by WAXS measurements demonstrated that PLLA block crystallizes first upon cooling from the melt, then the PCL block, and finally the PEO block. Except for the PLLA block (where the changes were not significant), both crystallization and melting temperatures of PCL and PEO decrease as the block content is lower in the terpolymers, which is expected in miscible or weakly segregated block copolymers.

The melt miscibility of the samples was confirmed by SAXS at 140 ºC. Both terpolymers exhibit a homogeneous melt morphology which is evidence of the miscibility of the three blocks in the melt. At room temperature, the morphology consists of alternating crystalline lamellae of each component with amorphous layers in between constituting novel triple crystalline spherulites (or axialites). Because PLLA crystallizes first, it affects the subsequent crystallization of PCL and later, both PLLA and PCL crystals restrict the crystallization of PEO. Therefore, the crystallization and melting enthalpies and characteristic temperatures of both PCL and PEO blocks decrease as their content is reduced.

PLLA block crystallization templates the morphology of the entire triblock terpolymer upon cooling from the melt. PLOM observations reveal that the morphology created by the PLLA block changes with composition. For the triblock terpolymer with a lower PLLA content, the superstructural morphology formed by the PLLA block resembles axialites.[62] But at higher PLLA content, the crystalline superstructure is more similar to spherulites. Upon further cooling from the melt, the crystallization of the PCL and PEO blocks do not alter the already formed superstructure, which acts as a template. Mixed spherulitic superstructures are formed and clear changes in the birefringence reflect the sequential crystallization of each block.

These triple crystalline PEO-*b*-PCL-*b*-PLLA terpolymers, with

novel mixed spherulites where three different types of lamellae coexist, offer new insights on the crystallization behavior of miscible block copolymers and further investigations will be pursued to access a better understanding of morphology and isothermal crystallization kinetics of these unique terpolymers as compared with their corresponding diblock and homopolymer precursors.

Acknowledgements

We gratefully acknowledge funds received through the following projects: "Mineco MAT2014-53437-C2-P", UPV/EHU (UFI 11/56) and GIC IT-586-13 (Basque Government).

References

1. N. Hadjichristidis, M. Pitsikalis and H. Iatrou, *Adv. Polym. Sci.*, 2005, **189**, 1-124.
2. S. Huang and S. Jiang, *RSC Advances*, 2014, **4**, 24566-24583.
3. M. J. Barthel, F. H. Schacher and U. S. Schubert, *Polym. Chem.*, 2014, **5**, 2647-2662.
4. R. M. Michell and A. J. Muller, *Prog. Polym. Sci.,* 2015**,** DOI: 10.1016/j.progpolymsci.2015.10.007.
5. S. Li and R. A. Register, in *Handbook of Polymer Crystallization*, eds. E. Piorkowska and G. C. Rutledge, John Wiley and Sons, Hoboken, New Jersey, 2013, ch. 11, pp. 327-346.
6. A. J. Müller, M. L. Arnal and A. T. Lorenzo, in *Handbook of Polymer Crystallization*, eds. E. Piorkowska and G. C. Rutledge, John Wiley and Sons, Hoboken, New Jersey, 2013, ch. 12, pp. 347-372.
7. R. V. Castillo and A. J. Müller, *Prog. Polym. Sci.*, 2009, **34**, 516-560.
8. A. J. Müller, V. Balsamo and M. L. Arnal, *Adv. Polym. Sci.*, 2005, **190**, 1-63.
9. A. J. Müller, M. L. Arnal and V. Balsamo, *Journal*, 2007, **714**, 229-259.
10. W. N. He and J. T. Xu, *Prog. Polym. Sci.*, 2012, **37**, 1350-1400.
11. M. Vivas, J. Contreras, F. López-Carrasquero, A. T. Lorenzo, M. L. Arnal, V. Balsamo, A. J. Müller, E. Laredo, H. Schmalz and V. Abetz, *Macromol. Sym.*, 2006, **239**, 58-67.
12. L. Sun, L. J. Shen, M. Q. Zhu, C. M. Dong and Y. Wei, *J. Polym. Sci., Part A: Polym. Chem.*, 2010, **48**, 4583-4593.
13. Y.-W. Chiang, Y.-Y. Hu, J.-N. Li, S.-H. Huang and S.-W. Kuo, *Macromolecules,* 2015**,** DOI: 10.1021/acs.macromol.5b02042.
14. C. Cai, L. U. Wang and C. M. Donc, *J. Polym. Sci., Part A: Polym. Chem.*, 2006, **44**, 2034-2044.
15. S. Vainionpää, P. Rokkanen and P. Törmälä, *Prog. Polym. Sci.*, 1989, **14**, 679-716.
16. R. M. Ho, P. Y. Hsieh, W. H. Tseng, C. C. Lin, B. H. Huang and B. Lotz, *Macromolecules*, 2003, **36**, 9085-9092.
17. J. K. Kim, D.-J. Park, M.-S. Lee and K. J. Ihn, *Polymer*, 2001, **42**, 7429-7441.
18. G. Maglio, A. Migliozzi and R. Palumbo, *Polymer*, 2003, **44**, 369-375.
19. O. Jeon, S. H. Lee, S. H. Kim, Y. M. Lee and Y. H. Kim, *Macromolecules*, 2003, **36**, 5585-5592.
20. I. W. Hamley, P. Parras, V. Castelletto, R. V. Castillo, A. J. Müller, E. Pollet, P. Dubois and C. M. Martin, *Macromol. Chem. Phys.*, 2006, **207**, 941-953.
21. I. W. Hamley, V. Castelletto, R. V. Castillo, A. J. Müller, C. M. Martin, E. Pollet and P. Dubois, *Macromolecules*, 2005, **38**, 463-472.
22. E. Laredo, N. Prutsky, A. Bello, M. Grimau, R. V. Castillo, A. J. Müller and P. Dubois, *Eur. Phys. J. E*, 2007, **23**, 295-303.
23. D. Kubies, F. Rypáček, J. Kovářová and F. Lednický, *Biomaterials*, 2000, **21**, 529-536.
24. L. Piao, Z. Dai, M. Deng, X. Chen and X. Jing, *Polymer*, 2003, **44**, 2025-2031.
25. C. He, J. Sun, C. Deng, T. Zhao, M. Deng, X. Chen and X. Jing, *Biomacromolecules*, 2004, **5**, 2042-2047.
26. C. He, J. Sun, T. Zhao, Z. Hong, X. Zhuang, X. Chen and X. Jing, *Biomacromolecules*, 2006, **7**, 252-258.
27. S. Nojima, M. Ono and T. Ashida, *Polym. J.*, 1992, **24**, 1271-1280.
28. L. Li, F. Meng, Z. Zhong, D. Byelov, W. H. De Jeu and J. Feijen, *J. Chem. Phys.*, 2007, **126**.
29. J. Sun, Z. Hong, L. Yang, Z. Tang, X. Chen and X. Jing, *Polymer*, 2004, **45**, 5969-5977.
30. S. M. Li, I. Rashkov, J. L. Espartero, N. Manolova and M. Vert, *Macromolecules*, 1996, **29**, 57-62.
31. K. S. Kim, S. Chung, I. J. Chin, M. N. Kim and J. S. Yoon, *J. Appl. Polym. Sci.*, 1999, **72**, 341-348.
32. D. W. Lim and T. G. Park, *J. Appl. Polym. Sci.*, 2000, **75**, 1615-1623.
33. C. He, J. Sun, J. Ma, X. Chen and X. Jing, *Biomacromolecules*, 2006, **7**, 3482-3489.
34. S. Jiang, C. He, L. An, X. Chen and B. Jiang, *Macromol. Chem. Phys.*, 2004, **205**, 2229-2234.
35. C. G. Mothé, W. S. Drumond and S. H. Wang, *Thermochim. Acta*, 2006, **445**, 61-66.
36. D. Shin, K. Shin, K. A. Aamer, G. N. Tew, T. P. Russell, J. H. Lee and J. Y. Jho, *Macromolecules*, 2005, **38**, 104-109.
37. Z. Wei, F. Yu, G. Chen, C. Qu, P. Wang, W. Zhang, J. Liang, M. Qi and L. Liu, *J. Appl. Polym. Sci.*, 2009, **114**, 1133-1140.
38. Z. Wei, L. Liu, F. Yu, P. Wang and M. Qi, *J. Appl. Polym. Sci.*, 2009, **111**, 429-436.
39. J. Yang, Y. Liang and C. C. Han, *Polymer (United Kingdom)*, 2015, **79**, 56-64.
40. J. Yang, Y. Liang, J. Luo, C. Zhao and C. C. Han, *Macromolecules*, 2012, **45**, 4254-4261.
41. B. Guillerm, V. Lemaur, B. Ernould, J. Cornil, R. Lazzaroni, J. F. Gohy, P. Dubois and O. Coulembier, *RSC Advances*, 2014, **4**, 10028-10038.
42. C. C. Liu, W. C. Chu, J. G. Li and S. W. Kuo, *Macromolecules*, 2014, **47**, 6389-6400.
43. J. Zhao, D. Pahovnik, Y. Gnanou and N. Hadjichristidis, *Polym. Chem.*, 2014, **5**, 3750-3753.
44. I. W. Hamley and V. Castelletto, *Prog. Polym. Sci.*, 2004, **29**, 909-948.
45. L. Leibler, *Macromolecules*, 1980, **13**, 1602-1617.
46. L. Peponi, I. Navarro-Baena, J. E. Báez, J. M. Kenny and A. Marcos-Fernández, *Polymer*, 2012, **53**, 4561-4568.
47. S. Huang, H. Li, S. Jiang, X. Chen and L. An, *Polym. Bull.*, 2011, **67**, 885-902.
48. I. W. Hamley, *The Physics of Block Copolymers*, Oxford University Press, Oxford 1998.
49. V. Abetz and P. F. W. Simon, *Adv. Polym. Sci.*, 2005, **189**, 125-212.
50. M. Rubinstein and R. H. Colby, *Polymer Physics*, OUP Oxford, 2003.
51. S. Huang, S. Jiang, L. An and X. Chen, *J. Polym. Sci., Part B: Polym. Phys.*, 2008, **46**, 1400-1411.

52. A. J. Muller, M. Avila, G. Saenz and J. Salazar, in *Poly(lactic acid) Science and Technology: Processing, Properties, Additives and Applications*, eds. A. Jimenez, M. Peltzer and R. Ruseckaite, The Royal Society of Chemistry, Cambridge, 2015, vol. 12, ch. 3, pp. 66-98.
53. J. L. Wang and C. M. Dong, *Macromol. Chem. Phys.*, 2006, **207**, 554-562.
54. R. V. Castillo, A. J. Müller, J. M. Raquez and P. Dubois, *Macromolecules*, 2010, **43**, 4149-4160.
55. J. R. Sarasua, R. E. Prud'homme, M. Wisniewski, A. Le Borgne and N. Spassky, *Macromolecules*, 1998, **31**, 3895-3905.
56. Y. Wang and J. F. Mano, *Eur. Polym. J.*, 2005, **41**, 2335-2342.
57. M. L. Di Lorenzo, *J. Appl. Polym. Sci.*, 2006, **100**, 3145-3151.
58. C. I. Huang, S. H. Tsai and C. M. Chen, *J. Polym. Sci., Part B: Polym. Phys.*, 2006, **44**, 2438-2448.
59. J. Zhang, K. Tashiro, H. Tsuji and A. J. Domb, *Macromolecules*, 2008, **41**, 1352-1357.
60. J. Sun, C. He, X. Zhuang, X. Jing and X. Chen, *J. Polym. Res.*, 2011, **18**, 2161-2168.
61. T. Scharf, *Polarized Light in Liquid Crystals and Polymers*, John Wiley & Sons Hoboken, New Jersey, 2007.
62. B. Crist, in *Handbook of Polymer Crystallization*, eds. E. Piorkowska and G. C. Rutledge, John Wiley and Sons, Hoboken, New Jersey, 2013, ch. 3, pp. 73-123.